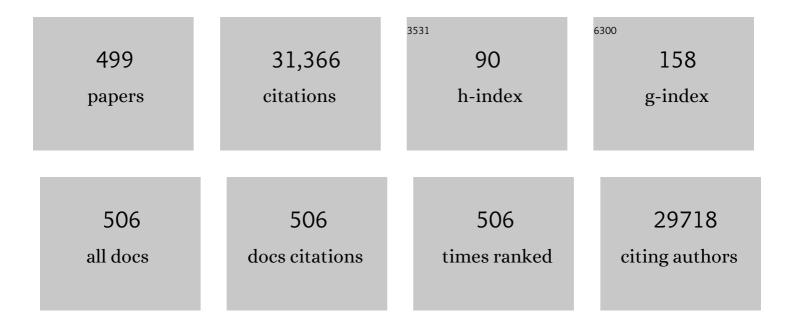
List of Publications by Year in descending order

Source: https://exaly.com/author-pdf/1355663/publications.pdf Version: 2024-02-01



#	Article	IF	CITATIONS
1	Experimental realization of two-dimensional boron sheets. Nature Chemistry, 2016, 8, 563-568.	13.6	1,398
2	Evidence of Silicene in Honeycomb Structures of Silicon on Ag(111). Nano Letters, 2012, 12, 3507-3511.	9.1	1,190
3	Exploring atomic defects in molybdenum disulphide monolayers. Nature Communications, 2015, 6, 6293.	12.8	1,124
4	Can Graphene be used as a Substrate for Raman Enhancement?. Nano Letters, 2010, 10, 553-561.	9.1	914
5	Evidence for Dirac Fermions in a Honeycomb Lattice Based on Silicon. Physical Review Letters, 2012, 109, 056804.	7.8	634
6	Graphdiyne: synthesis, properties, and applications. Chemical Society Reviews, 2019, 48, 908-936.	38.1	584
7	Synthesis of Graphdiyne Nanowalls Using Acetylenic Coupling Reaction. Journal of the American Chemical Society, 2015, 137, 7596-7599.	13.7	484
8	Raman Enhancement Effect on Two-Dimensional Layered Materials: Graphene, h-BN and MoS ₂ . Nano Letters, 2014, 14, 3033-3040.	9.1	464
9	Graphene as a Substrate To Suppress Fluorescence in Resonance Raman Spectroscopy. Journal of the American Chemical Society, 2009, 131, 9890-9891.	13.7	460
10	Graphene: A Platform for Surfaceâ€Enhanced Raman Spectroscopy. Small, 2013, 9, 1206-1224.	10.0	453
11	Robust Superhydrophobic Foam: A Graphdiyneâ€Based Hierarchical Architecture for Oil/Water Separation. Advanced Materials, 2016, 28, 168-173.	21.0	449
12	Water adsorption on metal surfaces: A general picture from density functional theory studies. Physical Review B, 2004, 69, .	3.2	448
13	Carbon Nanotubes and Related Nanomaterials: Critical Advances and Challenges for Synthesis toward Mainstream Commercial Applications. ACS Nano, 2018, 12, 11756-11784.	14.6	388
14	Dirac Fermions in Borophene. Physical Review Letters, 2017, 118, 096401.	7.8	353
15	Graphdiyne: A Metal-Free Material as Hole Transfer Layer To Fabricate Quantum Dot-Sensitized Photocathodes for Hydrogen Production. Journal of the American Chemical Society, 2016, 138, 3954-3957.	13.7	335
16	Doping-Free Fabrication of Carbon Nanotube Based Ballistic CMOS Devices and Circuits. Nano Letters, 2007, 7, 3603-3607.	9.1	319
17	Arrays of horizontal carbon nanotubes of controlled chirality grown using designed catalysts. Nature, 2017, 543, 234-238.	27.8	317
18	Identifying the Crystalline Orientation of Black Phosphorus Using Angleâ€Resolved Polarized Raman Spectroscopy. Angewandte Chemie - International Edition, 2015, 54, 2366-2369.	13.8	284

#	Article	IF	CITATIONS
19	Creation of Nanostructures with Poly(methyl methacrylate)-Mediated Nanotransfer Printing. Journal of the American Chemical Society, 2008, 130, 12612-12613.	13.7	283
20	Optical Anisotropy of Black Phosphorus in the Visible Regime. Journal of the American Chemical Society, 2016, 138, 300-305.	13.7	273
21	Carbon science in 2016: Status, challenges and perspectives. Carbon, 2016, 98, 708-732.	10.3	261
22	Nanoscale Chiral Rod-like Molecular Triads Assembled from Achiral Polyoxometalates. Journal of the American Chemical Society, 2010, 132, 14-15.	13.7	240
23	Vibrational Recognition of Hydrogen-Bonded Water Networks on a Metal Surface. Physical Review Letters, 2002, 89, 176104.	7.8	229
24	Growth of MoS _{2(1–<i>x</i>)} Se _{2<i>x</i>} (<i>x</i> = 0.41–1.00) Monolayer Alloys with Controlled Morphology by Physical Vapor Deposition. ACS Nano, 2015, 9, 7450-7455.	14.6	217
25	Large-Scale and Flexible Optical Synapses for Neuromorphic Computing and Integrated Visible Information Sensing Memory Processing. ACS Nano, 2021, 15, 1497-1508.	14.6	210
26	Two-Dimensional Molybdenum Tungsten Diselenide Alloys: Photoluminescence, Raman Scattering, and Electrical Transport. ACS Nano, 2014, 8, 7130-7137.	14.6	208
27	Firstâ€Layer Effect in Grapheneâ€Enhanced Raman Scattering. Small, 2010, 6, 2020-2025.	10.0	207
28	Synthesis of Hierarchical Graphdiyne-Based Architecture for Efficient Solar Steam Generation. Chemistry of Materials, 2017, 29, 5777-5781.	6.7	206
29	Spontaneous Symmetry Breaking and Dynamic Phase Transition in Monolayer Silicene. Physical Review Letters, 2013, 110, 085504.	7.8	205
30	Natural Dyes Adsorbed on TiO ₂ Nanowire for Photovoltaic Applications: Enhanced Light Absorption and Ultrafast Electron Injection. Nano Letters, 2008, 8, 3266-3272.	9.1	198
31	Ultrathin graphdiyne film on graphene through solution-phase van der Waals epitaxy. Science Advances, 2018, 4, eaat6378.	10.3	198
32	Effect of Graphene Fermi Level on the Raman Scattering Intensity of Molecules on Graphene. ACS Nano, 2011, 5, 5338-5344.	14.6	193
33	Real-time, local basis-set implementation of time-dependent density functional theory for excited state dynamics simulations. Journal of Chemical Physics, 2008, 129, 054110.	3.0	191
34	"Cloning―of Single-Walled Carbon Nanotubes via Open-End Growth Mechanism. Nano Letters, 2009, 9, 1673-1677.	9.1	191
35	Direct Synthesis of Graphdiyne Nanowalls on Arbitrary Substrates and Its Application for Photoelectrochemical Water Splitting Cell. Advanced Materials, 2017, 29, 1605308.	21.0	189
36	Controllable synthesis of brookite/anatase/rutile TiO2 nanocomposites and single-crystalline rutile nanorods array. Journal of Materials Chemistry, 2012, 22, 7937.	6.7	188

#	Article	IF	CITATIONS
37	Controlled Synthesis of ZrS ₂ Monolayer and Few Layers on Hexagonal Boron Nitride. Journal of the American Chemical Society, 2015, 137, 7051-7054.	13.7	178
38	Molecular Selectivity of Graphene-Enhanced Raman Scattering. Nano Letters, 2015, 15, 2892-2901.	9.1	177
39	Wrinkle-Free Single-Crystal Graphene Wafer Grown on Strain-Engineered Substrates. ACS Nano, 2017, 11, 12337-12345.	14.6	172
40	First Principles Design of Dye Molecules with Ullazine Donor for Dye Sensitized Solar Cells. Journal of Physical Chemistry C, 2013, 117, 3772-3778.	3.1	169
41	Telluriumâ€Assisted Epitaxial Growth of Largeâ€Area, Highly Crystalline ReS ₂ Atomic Layers on Mica Substrate. Advanced Materials, 2016, 28, 5019-5024.	21.0	169
42	Low-temperature growth and properties of ZnO nanowires. Applied Physics Letters, 2004, 84, 4941-4943.	3.3	163
43	DNA Nucleoside Interaction and Identification with Carbon Nanotubes. Nano Letters, 2007, 7, 45-50.	9.1	156
44	Direct evidence of metallic bands in a monolayer boron sheet. Physical Review B, 2016, 94, .	3.2	152
45	Graphdiyne: A Promising Catalyst–Support To Stabilize Cobalt Nanoparticles for Oxygen Evolution. ACS Catalysis, 2017, 7, 5209-5213.	11.2	150
46	Direct Growth of Semiconducting Single-Walled Carbon Nanotube Array. Journal of the American Chemical Society, 2009, 131, 14642-14643.	13.7	143
47	Synthesis and Applications of Graphdiyneâ€Based Metalâ€Free Catalysts. Advanced Materials, 2019, 31, e1803762.	21.0	143
48	Synthesis and electrical properties of carbon nanotube polyaniline composites. Applied Physics Letters, 2004, 85, 1796-1798.	3.3	142
49	Lighting Up the Raman Signal of Molecules in the Vicinity of Graphene Related Materials. Accounts of Chemical Research, 2015, 48, 1862-1870.	15.6	141
50	Electron and Hole Dynamics in Dye-Sensitized Solar Cells: Influencing Factors and Systematic Trends. Nano Letters, 2010, 10, 1238-1247.	9.1	137
51	Diatomiteâ€Templated Synthesis of Freestanding 3D Graphdiyne for Energy Storage and Catalysis Application. Advanced Materials, 2018, 30, e1800548.	21.0	134
52	Emergence of electron coherence and two-color all-optical switching in MoS ₂ based on spatial self-phase modulation. Proceedings of the National Academy of Sciences of the United States of America, 2015, 112, 11800-11805.	7.1	133
53	Robust Stacking-Independent Ultrafast Charge Transfer in MoS ₂ /WS ₂ Bilayers. ACS Nano, 2017, 11, 12020-12026.	14.6	130
54	Monitoring Local Strain Vector in Atomic-Layered MoSe ₂ by Second-Harmonic Generation. Nano Letters, 2017, 17, 7539-7543.	9.1	128

#	Article	IF	CITATIONS
55	Ordered and Reversible Hydrogenation of Silicene. Physical Review Letters, 2015, 114, 126101.	7.8	127
56	CMP Aerogels: Ultrahigh‧urfaceâ€Area Carbonâ€Based Monolithic Materials with Superb Sorption Performance. Advanced Materials, 2014, 26, 8053-8058.	21.0	125
57	2D graphdiyne materials: challenges and opportunities in energy field. Science China Chemistry, 2018, 61, 765-786.	8.2	123
58	Enhanced Raman Scattering on In-Plane Anisotropic Layered Materials. Journal of the American Chemical Society, 2015, 137, 15511-15517.	13.7	122
59	Chemical Alignment of Oxidatively Shortened Single-Walled Carbon Nanotubes on Silver Surface. Journal of Physical Chemistry B, 2001, 105, 5075-5078.	2.6	120
60	Growth of high-density horizontally aligned SWNT arrays using Trojan catalysts. Nature Communications, 2015, 6, 6099.	12.8	120
61	Graphene-Based Enhanced Raman Scattering toward Analytical Applications. Chemistry of Materials, 2016, 28, 6426-6435.	6.7	120
62	Correlations between Immobilizing Ions and Suppressing Hysteresis in Perovskite Solar Cells. ACS Energy Letters, 2016, 1, 266-272.	17.4	118
63	Raman Spectra and Corresponding Strain Effects in Graphyne and Graphdiyne. Journal of Physical Chemistry C, 2016, 120, 10605-10613.	3.1	116
64	Cap Formation Engineering: From Opened C ₆₀ to Single-Walled Carbon Nanotubes. Nano Letters, 2010, 10, 3343-3349.	9.1	115
65	Predicting Energy Conversion Efficiency of Dye Solar Cells from First Principles. Journal of Physical Chemistry C, 2014, 118, 16447-16457.	3.1	115
66	Architecture of βâ€Graphdiyneâ€Containing Thin Film Using Modified Glaser–Hay Coupling Reaction for Enhanced Photocatalytic Property of TiO ₂ . Advanced Materials, 2017, 29, 1700421.	21.0	115
67	Graphdiyne for crucial gas involved catalytic reactions in energy conversion applications. Energy and Environmental Science, 2020, 13, 1326-1346.	30.8	115
68	Controlled growth of large-area anisotropic ReS ₂ atomic layer and its photodetector application. Nanoscale, 2016, 8, 18956-18962.	5.6	114
69	Chemical Vapor Deposition Growth of Linked Carbon Monolayers with Acetylenic Scaffoldings on Silver Foil. Advanced Materials, 2017, 29, 1604665.	21.0	114
70	Few-Layer Graphene-Encapsulated Metal Nanoparticles for Surface-Enhanced Raman Spectroscopy. Journal of Physical Chemistry C, 2014, 118, 8993-8998.	3.1	113
71	Atomic Pd on Graphdiyne/Graphene Heterostructure as Efficient Catalyst for Aromatic Nitroreduction. Advanced Functional Materials, 2019, 29, 1905423.	14.9	112
72	Microscopic Dimensions Engineering: Stepwise Manipulation of the Surface Wettability on 3D Substrates for Oil/Water Separation. Advanced Materials, 2016, 28, 936-942.	21.0	109

#	Article	IF	CITATIONS
73	Solutionâ€Processable Highâ€Purity Semiconducting SWCNTs for Largeâ€Area Fabrication of Highâ€Performance Thinâ€Film Transistors. Small, 2016, 12, 4993-4999.	10.0	107
74	Quantum Mode Selectivity of Plasmon-Induced Water Splitting on Gold Nanoparticles. ACS Nano, 2016, 10, 5452-5458.	14.6	106
75	pH-Dependent Synthesis of Novel Structure-Controllable Polymer-Carbon NanoDots with High Acidophilic Luminescence and Super Carbon Dots Assembly for White Light-Emitting Diodes. ACS Applied Materials & Interfaces, 2016, 8, 4062-4068.	8.0	106
76	Probing the Effect of Molecular Orientation on the Intensity of Chemical Enhancement Using Grapheneâ€Enhanced Raman Spectroscopy. Small, 2012, 8, 1365-1372.	10.0	105
77	Raman Spectroscopy of Graphene. Acta Chimica Sinica, 2014, 72, 301.	1.4	105
78	Synthesis of Ultrathin Graphdiyne Film Using a Surface Template. ACS Applied Materials & Interfaces, 2019, 11, 2632-2637.	8.0	103
79	Theoretical Models of Eumelanin Protomolecules and their Optical Properties. Biophysical Journal, 2008, 94, 2095-2105.	0.5	100
80	Pyrolysis-induced synthesis of iron and nitrogen-containing carbon nanolayers modified graphdiyne nanostructure as a promising core-shell electrocatalyst for oxygen reduction reaction. Carbon, 2017, 119, 201-210.	10.3	99
81	Identifying the Crystalline Orientation of Black Phosphorus Using Angleâ€Resolved Polarized Raman Spectroscopy. Angewandte Chemie, 2015, 127, 2396-2399.	2.0	97
82	From Silicene to Half-Silicane by Hydrogenation. ACS Nano, 2015, 9, 11192-11199.	14.6	97
83	Nitrogenâ€Doped Carbon Nanotube Aerogels for Highâ€Performance ORR Catalysts. Small, 2015, 11, 3903-3908.	10.0	96
84	Side-group chemical gating via reversible optical and electric control in a single molecule transistor. Nature Communications, 2019, 10, 1450.	12.8	96
85	Sorting out Semiconducting Single-Walled Carbon Nanotube Arrays by Preferential Destruction of Metallic Tubes Using Xenon-Lamp Irradiation. Journal of Physical Chemistry C, 2008, 112, 3849-3856.	3.1	95
86	Interfaceâ€Engineered Plasmonics in Metal/Semiconductor Heterostructures. Advanced Energy Materials, 2016, 6, 1600431.	19.5	95
87	Superhydrophilic Graphdiyne Accelerates Interfacial Mass/Electron Transportation to Boost Electrocatalytic and Photoelectrocatalytic Water Oxidation Activity. Advanced Functional Materials, 2019, 29, 1808079.	14.9	95
88	Electricâ€Fieldâ€Assisted Growth of Vertical Graphene Arrays and the Application in Thermal Interface Materials. Advanced Functional Materials, 2020, 30, 2003302.	14.9	95
89	A universal etching-free transfer of MoS2 films for applications in photodetectors. Nano Research, 2015, 8, 3662-3672.	10.4	94
90	A new phase diagram of water under negative pressure: The rise of the lowest-density clathrate s-III. Science Advances, 2016, 2, e1501010.	10.3	92

#	Article	IF	CITATIONS
91	Design of a Photoactive Hybrid Bilayer Dielectric for Flexible Nonvolatile Organic Memory Transistors. ACS Nano, 2016, 10, 436-445.	14.6	91
92	Discovery of 2D Anisotropic Dirac Cones. Advanced Materials, 2018, 30, 1704025.	21.0	91
93	Surface-Enhanced Raman Scattering (SERS) from Azobenzene Self-Assembled "Sandwiches― Langmuir, 1999, 15, 16-19.	3.5	90
94	Suppressed superconductivity in substrate-supported <i>î²</i> ₁₂ borophene by tensile strain and electron doping. 2D Materials, 2017, 4, 025032.	4.4	90
95	Observation of Dirac Cone Warping and Chirality Effects in Silicene. ACS Nano, 2013, 7, 9049-9054.	14.6	88
96	The chemistry of organoimido derivatives of polyoxometalates. Dalton Transactions, 2012, 41, 3599.	3.3	87
97	Characterizing hydrophobicity of amino acid side chains in a protein environment via measuring contact angle of a water nanodroplet on planar peptide network. Proceedings of the National Academy of Sciences of the United States of America, 2016, 113, 12946-12951.	7.1	87
98	Interlayer‧tate oupling Dependent Ultrafast Charge Transfer in MoS ₂ /WS ₂ Bilayers. Advanced Science, 2017, 4, 1700086.	11.2	87
99	Graphdiyne/Graphene Heterostructure: A Universal 2D Scaffold Anchoring Monodispersed Transition-Metal Phthalocyanines for Selective and Durable CO ₂ Electroreduction. Journal of the American Chemical Society, 2021, 143, 8679-8688.	13.7	87
100	Macroscopic Carbon Nanotubeâ€based 3D Monoliths. Small, 2015, 11, 3263-3289.	10.0	83
101	Identifying sp–sp ² carbon materials by Raman and infrared spectroscopies. Physical Chemistry Chemical Physics, 2014, 16, 11303-11309.	2.8	81
102	Photoinduced Nonequilibrium Topological States in Strained Black Phosphorus. Physical Review Letters, 2018, 120, 237403.	7.8	80
103	Core-shell Ag@nitrogen-doped carbon quantum dots modified BiVO4 nanosheets with enhanced photocatalytic performance under Vis-NIR light: Synergism of molecular oxygen activation and surface plasmon resonance. Chemical Engineering Journal, 2021, 410, 128336.	12.7	79
104	Metastable phases of 2D boron sheets on Ag(1 1 1). Journal of Physics Condensed Matter, 2017, 29, 095002.	1.8	78
105	SnO ₂ @PANI Core–Shell Nanorod Arrays on 3D Graphite Foam: A High-Performance Integrated Electrode for Lithium-Ion Batteries. ACS Applied Materials & Interfaces, 2017, 9, 9620-9629.	8.0	78
106	Water printing of ferroelectric polarization. Nature Communications, 2018, 9, 3809.	12.8	75
107	Fast Growth of Strain-Free AlN on Graphene-Buffered Sapphire. Journal of the American Chemical Society, 2018, 140, 11935-11941.	13.7	75
108	Anomalous Polarized Raman Scattering and Large Circular Intensity Differential in Layered Triclinic ReS ₂ . ACS Nano, 2017, 11, 10366-10372.	14.6	74

#	Article	IF	CITATIONS
109	Horizontal Single-Walled Carbon Nanotube Arrays: Controlled Synthesis, Characterizations, and Applications. Chemical Reviews, 2020, 120, 12592-12684.	47.7	74
110	The Origin of Oxygen Vacancies Controlling La _{2/3} Sr _{1/3} MnO ₃ Electronic and Magnetic Properties. Advanced Materials Interfaces, 2016, 3, 1500753.	3.7	73
111	Enhanced tunable second harmonic generation from twistable interfaces and vertical superlattices in boron nitride homostructures. Science Advances, 2021, 7, .	10.3	73
112	State of the Art of Singleâ€Walled Carbon Nanotube Synthesis on Surfaces. Advanced Materials, 2014, 26, 5898-5922.	21.0	71
113	Diameter-Specific Growth of Semiconducting SWNT Arrays Using Uniform Mo2C Solid Catalyst. Journal of the American Chemical Society, 2015, 137, 8904-8907.	13.7	71
114	Spotting the differences in two-dimensional materials – the Raman scattering perspective. Chemical Society Reviews, 2018, 47, 3217-3240.	38.1	71
115	Influence of water on the electronic structure of metal-supported graphene: Insights from van der Waals density functional theory. Physical Review B, 2012, 85, .	3.2	70
116	Stacking-dependent electronic structure of bilayer silicene. Applied Physics Letters, 2014, 104, .	3.3	70
117	Atomic Disorders Induced by Silver and Magnesium Ion Migrations Favor High Thermoelectric Performance in αâ€MgAgSbâ€Based Materials. Advanced Functional Materials, 2015, 25, 6478-6488.	14.9	70
118	Chemical Vapor Deposition Growth of Single-Walled Carbon Nanotubes with Controlled Structures for Nanodevice Applications. Accounts of Chemical Research, 2014, 47, 2273-2281.	15.6	69
119	Density controlled oil uptake and beyond: from carbon nanotubes to graphene nanoribbon aerogels. Journal of Materials Chemistry A, 2015, 3, 20547-20553.	10.3	69
120	Epitaxial growth of large-area and highly crystalline anisotropic ReSe2 atomic layer. Nano Research, 2017, 10, 2732-2742.	10.4	69
121	Template Synthesis of an Ultrathin β-Graphdiyne-Like Film Using the Eglinton Coupling Reaction. ACS Applied Materials & Interfaces, 2019, 11, 2734-2739.	8.0	69
122	Structure–Property Relations in Allâ€Organic Dye‧ensitized Solar Cells. Advanced Functional Materials, 2013, 23, 424-429.	14.9	68
123	Microscopic Insight into Surface Wetting: Relations between Interfacial Water Structure and the Underlying Lattice Constant. Physical Review Letters, 2013, 110, 126101.	7.8	67
124	Z-scheme Ag3PO4/graphdiyne/g-C3N4 composites: Enhanced photocatalytic O2 generation benefiting from dual roles of graphdiyne. Carbon, 2018, 132, 598-605.	10.3	67
125	Exploring Approaches for the Synthesis of Few‣ayered Graphdiyne. Advanced Materials, 2019, 31, e1803758.	21.0	67
126	Integrated Plasmonics: Broadband Dirac Plasmons in Borophene. Physical Review Letters, 2020, 125, 116802.	7.8	67

#	Article	IF	CITATIONS
127	Nonâ€Volatile Electrolyteâ€Gated Transistors Based on Graphdiyne/MoS ₂ with Robust Stability for Lowâ€Power Neuromorphic Computing and Logicâ€Inâ€Memory. Advanced Functional Materials, 2021, 31, 2100069.	14.9	66
128	Modulating the Chargeâ€Transfer Enhancement in GERS using an Electrical Field under Vacuum and an n/pâ€Doping Atmosphere. Small, 2011, 7, 2945-2952.	10.0	65
129	Separation of Metallic and Semiconducting Singleâ€Walled Carbon Nanotube Arrays by "Scotch Tape― Angewandte Chemie - International Edition, 2011, 50, 6819-6823.	13.8	64
130	Photoexcitation in Solids: Firstâ€Principles Quantum Simulations by Realâ€Time TDDFT. Advanced Theory and Simulations, 2018, 1, 1800055.	2.8	64
131	Boron doped graphdiyne: A metal-free peroxidase mimetic nanozyme for antibacterial application. Nano Research, 2022, 15, 1446-1454.	10.4	64
132	Temperatureâ€Mediated Engineering of Graphdiyne Framework Enabling Highâ€Performance Potassium Storage. Advanced Functional Materials, 2020, 30, 2003039.	14.9	62
133	Field and temperature dependence of intrinsic diamagnetism in graphene: Theory and experiment. Physical Review B, 2015, 91, .	3.2	61
134	Growing highly pure semiconducting carbon nanotubes by electrotwisting the helicity. Nature Catalysis, 2018, 1, 326-331.	34.4	61
135	Determination of DNA-Base Orientation on Carbon Nanotubes through Directional Optical Absorbance. Nano Letters, 2007, 7, 2312-2316.	9.1	60
136	Nonlinear Rashba spin splitting in transition metal dichalcogenide monolayers. Nanoscale, 2016, 8, 17854-17860.	5.6	60
137	Growth of Close-Packed Semiconducting Single-Walled Carbon Nanotube Arrays Using Oxygen-Deficient TiO ₂ Nanoparticles as Catalysts. Nano Letters, 2015, 15, 403-409.	9.1	59
138	Chemical vapor deposition synthesis of near-zigzag single-walled carbon nanotubes with stable tube-catalyst interface. Science Advances, 2016, 2, e1501729.	10.3	59
139	Intelligent identification of two-dimensional nanostructures by machine-learning optical microscopy. Nano Research, 2018, 11, 6316-6324.	10.4	59
140	Designing Catalysts for Chiralityâ€5elective Synthesis of Singleâ€Walled Carbon Nanotubes: Past Success and Future Opportunity. Advanced Materials, 2019, 31, e1800805.	21.0	59
141	Birefringenceâ€Directed Raman Selection Rules in 2D Black Phosphorus Crystals. Small, 2016, 12, 2627-2633.	10.0	57
142	Electrostatic Functionalization and Passivation of Water-Exfoliated Few-Layer Black Phosphorus by Poly Dimethyldiallyl Ammonium Chloride and Its Ultrafast Laser Application. ACS Applied Materials & Interfaces, 2018, 10, 9679-9687.	8.0	57
143	Graphdiyne Filter for Decontaminating Leadâ€ŀonâ€Polluted Water. Advanced Electronic Materials, 2017, 3, 1700122.	5.1	56
144	Graphdiyne/Graphene/Graphdiyne Sandwiched Carbonaceous Anode for Potassium-Ion Batteries. ACS Nano, 2022, 16, 3163-3172.	14.6	56

#	Article	IF	CITATIONS
145	Bridging the Gap between Reality and Ideality of Graphdiyne: The Advances of Synthetic Methodology. CheM, 2020, 6, 1933-1951.	11.7	54
146	Catalystâ€Free Synthesis of Few‣ayer Graphdiyne Using a Microwaveâ€Induced Temperature Gradient at a Solid/Liquid Interface. Advanced Functional Materials, 2020, 30, 2001396.	14.9	54
147	Screening Magnetic Two-Dimensional Atomic Crystals with Nontrivial Electronic Topology. Journal of Physical Chemistry Letters, 2018, 9, 6709-6715.	4.6	53
148	Ultrafast charge ordering by self-amplified exciton–phonon dynamics in TiSe2. Nature Communications, 2020, 11, 43.	12.8	53
149	Charge-Transfer Plasmon Polaritons at Graphene/α-RuCl ₃ Interfaces. Nano Letters, 2020, 20, 8438-8445.	9.1	53
150	First-principles studies of cation-doped spinelLiMn2O4for lithium ion batteries. Physical Review B, 2003, 67, .	3.2	51
151	Novel Excitonic Solar Cells in Phosphorene–TiO ₂ Heterostructures with Extraordinary Charge Separation Efficiency. Journal of Physical Chemistry Letters, 2016, 7, 1880-1887.	4.6	51
152	Gas exfoliation of graphitic carbon nitride to improve the photocatalytic hydrogen evolution of metal-free 2D/2D g-C3N4/graphdiyne heterojunction. Journal of Alloys and Compounds, 2020, 833, 155054.	5.5	51
153	Superconductor–Insulator Transitions in Exfoliated Bi ₂ Sr ₂ CaCu ₂ O _{8+δ} Flakes. Nano Letters, 2018, 18, 5660-5665.	9.1	50
154	Transparent proton transport through a two-dimensional nanomesh material. Nature Communications, 2019, 10, 3971.	12.8	50
155	Gate-Tunable Reversible Rashba–Edelstein Effect in a Few-Layer Graphene/2H-TaS ₂ Heterostructure at Room Temperature. ACS Nano, 2020, 14, 5251-5259.	14.6	50
156	Giant enhancement of optical nonlinearity in two-dimensional materials by multiphoton-excitation resonance energy transfer from quantum dots. Nature Photonics, 2021, 15, 510-515.	31.4	50
157	New Pathway for Hot Electron Relaxation in Two-Dimensional Heterostructures. Nano Letters, 2018, 18, 6057-6063.	9.1	49
158	Transport behavior of water molecules through two-dimensional nanopores. Journal of Chemical Physics, 2014, 141, 18C528.	3.0	48
159	Temperature-dependent photoluminescence emission and Raman scattering from Mo _{1â^'<i>x</i>} W _{<i>x</i>} S ₂ monolayers. Nanotechnology, 2016, 27, 445705.	2.6	48
160	Unique structural advances of graphdiyne for energy applications. EnergyChem, 2020, 2, 100041.	19.1	48
161	Bimetallic Catalysts for the Efficient Growth of SWNTs on Surfaces. Chemistry of Materials, 2004, 16, 799-805.	6.7	47
162	Sorting out semiconducting single-walled carbon nanotube arrays by preferential destruction of metallic tubes using water. Journal of Materials Chemistry, 2011, 21, 11815.	6.7	47

#	Article	IF	CITATIONS
163	"Snowing―Graphene using Microwave Ovens. Advanced Materials, 2018, 30, e1803189.	21.0	47
164	Growth of Horizontal Semiconducting SWNT Arrays with Density Higher than 100 tubes/μm using Ethanol/Methane Chemical Vapor Deposition. Journal of the American Chemical Society, 2016, 138, 6727-6730.	13.7	46
165	Anisotropic Strain Relaxation of Graphene by Corrugation on Copper Crystal Surfaces. Small, 2018, 14, e1800725.	10.0	46
166	Toward the Chemistry of Carboxylic Single-Walled Carbon Nanotubes by Chemical Force Microscopy. Journal of Physical Chemistry B, 2002, 106, 4139-4144.	2.6	45
167	Helicity-dependent single-walled carbon nanotube alignment on graphite for helical angle and handedness recognition. Nature Communications, 2013, 4, 2205.	12.8	45
168	Ideal type-II Weyl phonons in wurtzite Cul. Physical Review B, 2019, 100, .	3.2	45
169	Water adsorption on a NaCl (001) surface: A density functional theory study. Physical Review B, 2006, 74, .	3.2	43
170	Synthesis of Hydrogen‧ubstituted Graphyne Film for Lithium–Sulfur Battery Applications. Small, 2019, 15, 1805344.	10.0	42
171	Growth kinetics of single-walled carbon nanotubes with a (2 <i>n</i> , <i>n</i>) chirality selection. Science Advances, 2019, 5, eaav9668.	10.3	42
172	Modeling charge recombination in dye-sensitized solar cells using first-principles electron dynamics: effects of structural modification. Physical Chemistry Chemical Physics, 2013, 15, 17187.	2.8	41
173	In Situ Quantitative Graphene-Based Surface-Enhanced Raman Spectroscopy. Small Methods, 2017, 1, 1700126.	8.6	41
174	Pristine organo-imido polyoxometalates as an anode for lithium ion batteries. RSC Advances, 2014, 4, 7374.	3.6	40
175	Lattice thermal conductivity including phonon frequency shifts and scattering rates induced by quartic anharmonicity in cubic oxide and fluoride perovskites. Physical Review B, 2021, 104, .	3.2	40
176	Theoretical Insights into Ultrafast Dynamics in Quantum Materials. Ultrafast Science, 2022, 2022, .	11.2	40
177	Mechanisms for Ultrafast Nonradiative Relaxation in Electronically Excited Eumelanin Constituents. Biophysical Journal, 2008, 95, 4396-4402.	0.5	39
178	The effect of moiré superstructures on topological edge states in twisted bismuthene homojunctions. Science Advances, 2020, 6, eaba2773.	10.3	39
179	Iron Catalysts Reactivation for Efficient CVD Growth of SWNT with Base-growth Mode on Surface. Journal of Physical Chemistry B, 2004, 108, 12665-12668.	2.6	38
180	Crinkling Ultralong Carbon Nanotubes into Serpentines by a Controlled Landing Process. Advanced Materials, 2009, 21, 4158-4162.	21.0	38

#	Article	IF	CITATIONS
181	Selective Scission of C–O and C–C Bonds in Ethanol Using Bimetal Catalysts for the Preferential Growth of Semiconducting SWNT Arrays. Journal of the American Chemical Society, 2015, 137, 1012-1015.	13.7	38
182	Controllable Growth of (n, n â^'1) Family of Semiconducting Carbon Nanotubes. CheM, 2019, 5, 1182-1193.	11.7	38
183	Dual-gated single-molecule field-effect transistors beyond Moore's law. Nature Communications, 2022, 13, 1410.	12.8	38
184	Selective adsorption and electronic interaction ofF16CuPcon epitaxial graphene. Physical Review B, 2010, 82, .	3.2	37
185	Superconductivity in dense carbon-based materials. Physical Review B, 2016, 93, .	3.2	37
186	3D Self‣upporting Porous Magnetic Assemblies for Water Remediation and Beyond. Advanced Energy Materials, 2016, 6, 1600473.	19.5	37
187	Lattice Vibration and Raman Scattering in Anisotropic Black Phosphorus Crystals. Small Methods, 2018, 2, 1700409.	8.6	37
188	Effect of Cation–π Interaction on Macroionic Selfâ€Assembly. Angewandte Chemie - International Edition, 2018, 57, 4067-4072.	13.8	37
189	Plasmon-Induced Ultrafast Hydrogen Production in Liquid Water. Journal of Physical Chemistry Letters, 2018, 9, 63-69.	4.6	37
190	Probing Nonequilibrium Dynamics of Photoexcited Polarons on a Metal-Oxide Surface with Atomic Precision. Physical Review Letters, 2020, 124, 206801.	7.8	37
191	Observation of Topological Flat Bands in the Kagome Semiconductor Nb ₃ Cl ₈ . Nano Letters, 2022, 22, 4596-4602.	9.1	37
192	Large-area growth of ultra-high-density single-walled carbon nanotube arrays on sapphire surface. Nano Research, 2015, 8, 3694-3703. Quartic anharmonicity and anomalous thermal conductivity in cubic antipercyspites combination.	10.4	36
193	xmlns:mml="http://www.w3.org/1998/Math/MathML"> <mml:mrow><mml:msub><mml:mi>A</mml:mi><mml:m mathvariant="normal">O</mml:m </mml:msub></mml:mrow> <mml:math< td=""><td>ın>3<td>l:mn> </td></td></mml:math<>	ın>3 <td>l:mn> </td>	l:mn>

#	Article	IF	CITATIONS
199	Depth-dependent valence stratification driven by oxygen redox in lithium-rich layered oxide. Nature Communications, 2020, 11, 6342.	12.8	34
200	Synthesis of wafer-scale ultrathin graphdiyne for flexible optoelectronic memory with over 256 storage levels. CheM, 2021, 7, 1284-1296.	11.7	34
201	display="inline"> <mml:mrow><mml:mi>s</mml:mi></mml:mrow> -Wave Pairing in Josephson Junctions Made of Twisted Ultrathin <mml:math xmlns:mml="http://www.w3.org/1998/Math/MathML" display="inline"><mml:mrow><mml:mrow><mml:mrow><mml:mi>Bi</mml:mi></mml:mrow><mml:mrow><mml:mrow><mml:mrow><mml:mrow><mml:mrow><mml:mrow><mml:mrow><mml:mrow><mml:mrow><mml:mrow><mml:mrow><mml:mrow><mml:mrow><mml:mrow><mml:mrow><mml:mrow><mml:mrow><mml:mrow><mml:mrow><mml:mrow><mml:mrow><mml:mrow><mml:mrow><mml:mrow><mml:mrow><mml:mrow><mml:mrow><mml:mrow><mml:mrow><mml:mrow><mml:mrow><mml:mrow><mml:mrow><mml:mrow><mml:mrow><mml:mrow><mml:mrow><mml:mrow><mml:mrow><mml:mrow><mml:mrow><mml:mrow><mml:mrow><mml:mrow><mml:mrow><mml:mrow><mml:mrow><mml:mrow><mml:mrow><mml:mrow><mml:mrow><mml:mrow><mml:mrow><mml:mrow><mml:mrow><mml:mrow><mml:mrow><mml:mrow><mml:mrow><mml:mrow><mml:mrow><mml:mrow><mml:mrow><mml:mrow><mml:mrow><mml:mrow><mml:mrow><mml:mrow><mml:mrow><mml:mrow><mml:mrow><mml:mrow><mml:mrow><mml:mrow><mml:mrow><mml:mrow><mml:mrow><mml:mrow><mml:mrow><mml:mrow><mml:mrow><mml:mrow><mml:mrow><mml:mrow><mml:mrow><mml:mrow><mml:mrow><mml:mrow><mml:mrow><mml:mrow><mml:mrow><mml:mrow><mml:mrow><mml:mrow><mml:mrow><mml:mrow><mml:mrow><mml:mrow><mml:mrow><mml:mrow><mml:mrow><mml:mrow><mml:mrow><mml:mrow><mml:mrow><mml:mrow><mml:mrow><mml:mrow><mml:mrow><mml:mrow><mml:mrow><mml:mrow><mml:mrow><mml:mrow><mml:mrow><mml:mrow><mml:mrow><mml:mrow><mml:mrow><mml:mrow><mml:mrow><mml:mrow><mml:mrow><mml:mrow><mml:mrow><mml:mrow><mml:mrow><mml:mrow><mml:mrow><mml:mrow><mml:mrow><mml:mrow><mml:mrow><mml:mrow><mml:mrow><mml:mrow><mml:mrow><mml:mrow><mml:mrow><mml:mrow><mml:mrow><mml:mrow><mml:mrow><mml:mrow><mml:mrow><mml:mrow><mml:mrow><mml:mrow><mml:mrow><mml:mrow><mml:mrow><mml:mrow><mml:mrow><mml:mrow><mml:mrow><mml:mrow><mml:mrow><mml:mrow><mml:mrow><mml:mrow><mml:mrow><mml:mrow><mml:mrow><mml:mrow><mml:mrow><mml:mrow><mml:mrow><mml:mrow><mml:mrow><mml:mrow><mml:mrow><mml:mrow><mml:mrow><mml:mrow><mml:mrow><mml:mrow><mml:mrow><mml:mrow><</mml:mrow></mml:mrow></mml:mrow></mml:mrow></mml:mrow></mml:mrow></mml:mrow></mml:mrow></mml:mrow></mml:mrow></mml:mrow></mml:mrow></mml:mrow></mml:mrow></mml:mrow></mml:mrow></mml:mrow></mml:mrow></mml:mrow></mml:mrow></mml:mrow></mml:mrow></mml:mrow></mml:mrow></mml:mrow></mml:mrow></mml:mrow></mml:mrow></mml:mrow></mml:mrow></mml:mrow></mml:mrow></mml:mrow></mml:mrow></mml:mrow></mml:mrow></mml:mrow></mml:mrow></mml:mrow></mml:mrow></mml:mrow></mml:mrow></mml:mrow></mml:mrow></mml:mrow></mml:mrow></mml:mrow></mml:mrow></mml:mrow></mml:mrow></mml:mrow></mml:mrow></mml:mrow></mml:mrow></mml:mrow></mml:mrow></mml:mrow></mml:mrow></mml:mrow></mml:mrow></mml:mrow></mml:mrow></mml:mrow></mml:mrow></mml:mrow></mml:mrow></mml:mrow></mml:mrow></mml:mrow></mml:mrow></mml:mrow></mml:mrow></mml:mrow></mml:mrow></mml:mrow></mml:mrow></mml:mrow></mml:mrow></mml:mrow></mml:mrow></mml:mrow></mml:mrow></mml:mrow></mml:mrow></mml:mrow></mml:mrow></mml:mrow></mml:mrow></mml:mrow></mml:mrow></mml:mrow></mml:mrow></mml:mrow></mml:mrow></mml:mrow></mml:mrow></mml:mrow></mml:mrow></mml:mrow></mml:mrow></mml:mrow></mml:mrow></mml:mrow></mml:mrow></mml:mrow></mml:mrow></mml:mrow></mml:mrow></mml:mrow></mml:mrow></mml:mrow></mml:mrow></mml:mrow></mml:mrow></mml:mrow></mml:mrow></mml:mrow></mml:mrow></mml:mrow></mml:mrow></mml:mrow></mml:mrow></mml:mrow></mml:mrow></mml:mrow></mml:mrow></mml:mrow></mml:mrow></mml:mrow></mml:mrow></mml:mrow></mml:mrow></mml:mrow></mml:mrow></mml:mrow></mml:mrow></mml:mrow></mml:mrow></mml:mrow></mml:mrow></mml:mrow></mml:mrow></mml:mrow></mml:mrow></mml:mrow></mml:mrow></mml:mrow></mml:mrow></mml:mrow></mml:mrow></mml:mrow></mml:mrow></mml:mrow></mml:mrow></mml:mrow></mml:mrow></mml:mrow></mml:mrow></mml:mrow></mml:mrow></mml:mrow></mml:mrow></mml:mrow></mml:mrow></mml:mrow></mml:mrow></mml:mrow></mml:mrow></mml:mrow></mml:mrow></mml:mrow></mml:mrow></mml:mrow></mml:mrow></mml:mrow></mml:mrow></mml:mrow></mml:mrow></mml:mrow></mml:mrow></mml:math 	8.9 :mn>2 <td>34 iml:mn></td>	34 iml:mn>
202	Physical Review X, 2021, 11, . The proton-controlled synthesis of unprecedented diol functionalized Anderson-type POMs. Chemical Communications, 2016, 52, 2378-2381.	4.1	33
203	Theoretical investigation of the C60/copper phthalocyanine organic photovoltaic heterojunction. Nano Research, 2012, 5, 248-257.	10.4	32
204	Rational design of three-dimensional nitrogen-doped carbon nanoleaf networks for high-performance oxygen reduction. Journal of Materials Chemistry A, 2015, 3, 5617-5627.	10.3	32
205	<i>Ab initio</i> evidence for nonthermal characteristics in ultrafast laser melting. Physical Review B, 2016, 94, .	3.2	32
206	Hybrid-dimensional magnetic microstructure based 3D substrates for remote controllable and ultrafast water remediation. Journal of Materials Chemistry A, 2016, 4, 938-943.	10.3	32
207	SWCNTâ€MoS ₂ â€SWCNT Vertical Point Heterostructures. Advanced Materials, 2017, 29, 1604469.	21.0	32
208	Ultrafast Catalyst-Free Graphene Growth on Glass Assisted by Local Fluorine Supply. ACS Nano, 2019, 13, 10272-10278.	14.6	32
209	Differentiated Visualization of Single-Cell 5-Hydroxymethylpyrimidines with Microfluidic Hydrogel Encoding. Journal of the American Chemical Society, 2020, 142, 2889-2896.	13.7	32
210	Photoexcitation Induced Quantum Dynamics of Charge Density Wave and Emergence of a Collective Mode in 1 <i>T</i> -TaS ₂ . Nano Letters, 2019, 19, 6027-6034.	9.1	31
211	Graphene Oxide "Surfactantâ€â€Directed Tunable Concentration of Graphene Dispersion. Small, 2020, 16, e2003426.	10.0	31
212	Ultrafast Optical Modulation of Harmonic Generation in Two-Dimensional Materials. Nano Letters, 2020, 20, 8053-8058.	9.1	31
213	Chen <i>etÂal.</i> Reply:. Physical Review Letters, 2013, 110, 229702.	7.8	30
214	Scalable Fabrication of Ambipolar Transistors and Radioâ€Frequency Circuits Using Aligned Carbon Nanotube Arrays. Advanced Materials, 2014, 26, 645-652.	21.0	30
215	Sharp-Tip Silver Nanowires Mounted on Cantilevers for High-Aspect-Ratio High-Resolution Imaging. Nano Letters, 2016, 16, 6896-6902.	9.1	30
216	Ultrathermostable, Magnetic-Driven, and Superhydrophobic Quartz Fibers for Water Remediation. ACS Applied Materials & Interfaces, 2016, 8, 1025-1032.	8.0	30

#	Article	IF	CITATIONS
217	Recycling Strategy for Fabricating Low-Cost and High-Performance Carbon Nanotube TFT Devices. ACS Applied Materials & Interfaces, 2017, 9, 15719-15726.	8.0	30
218	Rapid Synthesis of Graphdiyne Films on Hydrogel at the Superspreading Interface for Antibacteria. ACS Nano, 2022, 16, 11338-11345.	14.6	30
219	Quantum plasmonics: Symmetry-dependent plasmon-molecule coupling and quantized photoconductances. Physical Review B, 2012, 86, .	3.2	29
220	Photocontrol of charge injection/extraction at electrode/semiconductor interfaces for high-photoresponsivity organic transistors. Journal of Materials Chemistry C, 2016, 4, 5289-5296.	5.5	29
221	Inâ€Plane Uniaxial Strain in Black Phosphorus Enables the Identification of Crystalline Orientation. Small, 2017, 13, 1700466.	10.0	29
222	Ultrafast Broadband Charge Collection from Clean Graphene/CH ₃ NH ₃ PbI ₃ Interface. Journal of the American Chemical Society, 2018, 140, 14952-14957.	13.7	29
223	Electronic Structures and Catalytic Activities of Niobium Oxides as Electrocatalysts in Liquidâ€Junction Photovoltaic Devices. Solar Rrl, 2020, 4, 1900430.	5.8	29
224	Optical Control of Multistage Phase Transition via Phonon Coupling in <mml:math xmlns:mml="http://www.w3.org/1998/Math/MathML" display="inline"><mml:mrow><mml:msub><mml:mrow><mml:mi>MoTe</mml:mi></mml:mrow><mml:mrow><n Physical Review Letters, 2022, 128, 015702.</n </mml:mrow></mml:msub></mml:mrow></mml:math 	nml:mn>2	: <del 29 : </td
225	Multilayered silicene: the bottom-up approach for a weakly relaxed Si(111) with Dirac surface states. Nanoscale, 2015, 7, 15880-15885.	5.6	28
226	Recent progresses in real-time local-basis implementation of time dependent density functional theory for electron–nucleus dynamics. Computational Materials Science, 2016, 112, 478-486.	3.0	28
227	Graphdiyne Nanowall for Enhanced Photoelectrochemical Performance of Si Heterojunction Photoanode. ACS Applied Materials & Interfaces, 2019, 11, 2745-2749.	8.0	28
228	Two-gap and three-gap superconductivity in <mml:math xmlns:mml="http://www.w3.org/1998/Math/MathML"><mml:msub><mml:mi>AlB</mml:mi><mml:mn>2-based films. Physical Review B, 2019, 100, .</mml:mn></mml:msub></mml:math 	nn 3.2/ mml:	:m 28 b>
229	Spin-Orientation-Dependent Topological States in Two-Dimensional Antiferromagnetic NiTl ₂ S ₄ Monolayers. Nano Letters, 2019, 19, 3321-3326.	9.1	28
230	Flat AgTe Honeycomb Monolayer on Ag(111). Journal of Physical Chemistry Letters, 2019, 10, 1866-1871.	4.6	28
231	Vertically Aligned Graphene for Thermal Interface Materials. Small Structures, 2020, 1, 2000034.	12.0	28
232	Polarized Raman Spectroscopy for Determining Crystallographic Orientation of Low-Dimensional Materials. Journal of Physical Chemistry Letters, 2021, 12, 7442-7452.	4.6	28
233	Effective Hamiltonian for FeAs-based superconductors. Physical Review B, 2008, 78, .	3.2	27
234	Grow Single-Walled Carbon Nanotubes Cross-Bar in One Batch. Journal of Physical Chemistry C, 2009, 113, 5341-5344.	3.1	27

#	Article	IF	CITATIONS
235	Basic science of water: Challenges and current status towards a molecular picture. Nano Research, 2015, 8, 3085-3110.	10.4	27
236	Identifying and Modulating Accidental Fermi Resonance: 2D IR and DFT Study of 4-Azido- <scp>l</scp> -phenylalanine. Journal of Physical Chemistry B, 2018, 122, 8122-8133.	2.6	27
237	Sub-10 nm Monolayer MoS ₂ Transistors Using Single-Walled Carbon Nanotubes as an Evaporating Mask. ACS Applied Materials & Interfaces, 2019, 11, 11612-11617.	8.0	27
238	An Ultrafast Nonvolatile Memory with Low Operation Voltage for Highâ€Speed and Lowâ€Power Applications. Advanced Functional Materials, 2021, 31, 2102571.	14.9	27
239	xmlns:mml="http://www.w3.org/1998/Math/MathML" display="inline"> <mml:mrow><mml:mn>1</mml:mn><mml:mi mathvariant="normal">T<mml:mtext>â[^]</mml:mtext><mml:mi>Ta</mml:mi><mml:msub><mml:mrow mathvariant="normal">S</mml:mrow </mml:msub></mml:mi </mml:mrow> <mml:mrow><mml:mn>2</mml:mn></mml:mrow>	7.8 > <mml:mi <td>27 :ow></td></mml:mi 	27 :ow>
240	Physical Review Letters, 2021, 126, 196406. Sorting out Semiconducting Singleâ€Walled Carbon Nanotube Arrays by Washing off Metallic Tubes Using SDS Aqueous Solution. Small, 2013, 9, 1306-1311.	10.0	26
241	Direct measurement of the Raman enhancement factor of rhodamine 6G on graphene under resonant excitation. Nano Research, 2014, 7, 1271-1279.	10.4	26
242	High thermopower and potential thermoelectric properties of crystalline LiH and NaH. Physical Review B, 2017, 95, .	3.2	26
243	Superstructure-Induced Splitting of Dirac Cones in Silicene. Physical Review Letters, 2019, 122, 196801.	7.8	26
244	Highly Potassiophilic Graphdiyne Skeletons Decorated with Cu Quantum Dots Enable Dendriteâ€Free Potassiumâ€Metal Anodes. Advanced Materials, 2022, 34, e2202685.	21.0	26
245	Enrichment of metallic carbon nanotubes by electric field-assisted chemical vapor deposition. Carbon, 2011, 49, 2555-2560.	10.3	25
246	Exotic thermoelectric behavior in nitrogenated holey graphene. RSC Advances, 2017, 7, 25803-25810.	3.6	25
247	Effects of line defects on the electronic and optical properties of strain-engineered WO ₃ thin films. Journal of Materials Chemistry C, 2017, 5, 11694-11699.	5.5	25
248	Universal Scaling of Intrinsic Resistivity in Twoâ€Dimensional Metallic Borophene. Angewandte Chemie - International Edition, 2018, 57, 4585-4589.	13.8	25
249	Identifying Few-Molecule Water Clusters with High Precision on Au(111) Surface. ACS Nano, 2018, 12, 6452-6457.	14.6	25
250	Water transport through subnanopores in the ultimate size limit: Mechanism from molecular dynamics. Nano Research, 2019, 12, 587-592.	10.4	25
251	Manipulating Weyl quasiparticles by orbital-selective photoexcitation in WTe2. Nature Communications, 2021, 12, 1885.	12.8	25
252	Graphene: A promising candidate for charge regulation in high-performance lithium-ion batteries. Nano Research, 2021, 14, 4370-4385.	10.4	25

#	Article	IF	CITATIONS
253	Building a Bridge for Carbon Nanotubes from Nanoscale Structure to Macroscopic Application. Journal of the American Chemical Society, 2021, 143, 18805-18819.	13.7	25
254	Thermoelectric performance in the binary semiconductor compound <mml:math xmlns:mml="http://www.w3.org/1998/Math/MathML"><mml:mrow><mml:msub><mml:mi>A</mml:mi>width="4pt" /><mml:mo>(</mml:mo><mml:mi>A</mml:mi> //mml:math> = K, Rb) with host-guest structure. Physical Review B, 2022, 105, .</mml:msub></mml:mrow></mml:math>	1>23.2	mn> 25 </td
255	Nanometer-Scale Lateral p–n Junctions in Graphene/α-RuCl ₃ Heterostructures. Nano Letters, 2022, 22, 1946-1953.	9.1	25
256	Evaluating Bandgap Distributions of Carbon Nanotubes via Scanning Electron Microscopy Imaging of the Schottky Barriers. Nano Letters, 2013, 13, 5556-5562.	9.1	24
257	Linear Dichroism and Nondestructive Crystalline Identification of Anisotropic Semimetal Fewâ€Layer MoTe ₂ . Small, 2019, 15, e1903159.	10.0	24
	Cooperative evolution of intraband and interband excitations for high-harmonic generation in strained <mml:math< td=""><td></td><td></td></mml:math<>		
258	xmlns:mml="http://www.w3.org/1998/Math/MathML"> <mml:msub><mml:mi>MoS</mml:mi><mml:mn>2Physical Review B, 2019, 99, .</mml:mn></mml:msub>	:m <mark>3;2</mark> <td>ıl:msub></td>	ıl:msub>
259	Anomalous electronic and thermoelectric transport properties in cubic <mml:math xmlns:mml="http://www.w3.org/1998/Math/MathML"><mml:mrow><mml:msub><mml:mi>Rb</mml:mi><mml:n antiperovskite. Physical Review B, 2020, 102, .</mml:n </mml:msub></mml:mrow></mml:math 	າກ ଃ3 ∝/mm	l :r⊉ #>
260	Indirect to Direct Charge Transfer Transition in Plasmonâ€Enabled CO ₂ Photoreduction. Advanced Science, 2022, 9, e2102978.	11.2	24
261	Soft-lock drawing of super-aligned carbon nanotube bundles for nanometre electrical contacts. Nature Nanotechnology, 2022, 17, 278-284.	31.5	24
262	Band Engineering of Carbon Nanotubes for Device Applications. Matter, 2020, 3, 664-695.	10.0	23
263	Graphdiyne Coupled with g ₃ N ₄ /NiFe‣ayered Double Hydroxide, a Layered Nanohybrid for Highly Efficient Photoelectrochemical Water Oxidation. Advanced Materials Interfaces, 2020, 7, 1902083.	3.7	23
264	Ultrahigh secondary electron emission of carbon nanotubes. Applied Physics Letters, 2010, 96, .	3.3	22
265	Selective Growth of Subnanometer Diameter Single-Walled Carbon Nanotube Arrays in Hydrogen-Free CVD. Journal of the American Chemical Society, 2016, 138, 12723-12726.	13.7	22
266	Origin of Improved Optical Quality of Monolayer Molybdenum Disulfide Grown on Hexagonal Boron Nitride Substrate. Small, 2016, 12, 198-203.	10.0	22
	Prediction of two-dimensional electron gas mediated magnetoelectric coupling at ferroelectric <mml:math< td=""><td></td><td></td></mml:math<>		
267	xmlns:mml="http://www.w3.org/1998/Math/MathML"> <mml:mrow><mml:msub><mml:mi>PbTiO</mml:mi><mr heterostructures. Physical Review B. 2017. 95</mr </mml:msub></mml:mrow>	nl:mn>3 </td <td>mm1:mn></td>	mm1:mn>
268	Nonadiabatic Dynamics of Photocatalytic Water Splitting on A Polymeric Semiconductor. Nano Letters, 2021, 21, 6449-6455.	9.1	22
269	Precise replication of antireflective nanostructures from biotemplates. Applied Physics Letters, 2007, 90, 123115.	3.3	21
270	A photodegradable hexaaza-pentacene molecule for selective dispersion of large-diameter semiconducting carbon nanotubes. Chemical Communications, 2016, 52, 7683-7686.	4.1	21

#	Article	IF	CITATIONS
271	Carbonâ€Nanotubeâ€Confined Vertical Heterostructures with Asymmetric Contacts. Advanced Materials, 2017, 29, 1702942.	21.0	21
272	Microwaveâ€Assisted Regeneration of Singleâ€Walled Carbon Nanotubes from Carbon Fragments. Small, 2018, 14, e1800033.	10.0	21
273	Momentum-resolved TDDFT algorithm in atomic basis for real time tracking of electronic excitation. Journal of Chemical Physics, 2018, 149, 154104.	3.0	21
274	Characterization of Excitonic Nature in Raman Spectra Using Circularly Polarized Light. ACS Nano, 2020, 14, 10527-10535.	14.6	21
275	Growth of Singleâ€Walled Carbon Nanotubes with Controlled Structure: Floating Carbide Solid Catalysts. Angewandte Chemie - International Edition, 2020, 59, 10884-10887.	13.8	21
276	Water wettability of close-packed metal surfaces. Journal of Chemical Physics, 2007, 127, 244710.	3.0	20
277	Carbene-mediated self-assembly of diamondoids on metal surfaces. Nanoscale, 2016, 8, 8966-8975.	5.6	20
278	An Iron-Porphyrin Complex with Large Easy-Axis Magnetic Anisotropy on Metal Substrate. ACS Nano, 2017, 11, 11402-11408.	14.6	20
279	Dirac cone pairs in silicene induced by interface Si-Ag hybridization: A first-principles effective band study. Physical Review B, 2017, 95, .	3.2	20
280	Hexagonal Monolayer Ice without Shared Edges. Physical Review Letters, 2018, 121, 256001.	7.8	20
281	Electrical control of spatial resolution in mixed-dimensional heterostructured photodetectors. Proceedings of the National Academy of Sciences of the United States of America, 2019, 116, 6586-6593.	7.1	20
282	Advance in Closeâ€Edged Graphene Nanoribbon: Property Investigation and Structure Fabrication. Small, 2019, 15, e1804473.	10.0	20
283	Continuous "Snowing―Thermotherapeutic Graphene. Advanced Materials, 2020, 32, e2002024.	21.0	20
284	Monolayer puckered pentagonal VTe2: An emergent two-dimensional ferromagnetic semiconductor with multiferroic coupling. Nano Research, 2022, 15, 1486-1491.	10.4	20
285	Photoluminescence Recovery from Single-Walled Carbon Nanotubes on Substrates. Journal of the American Chemical Society, 2007, 129, 12382-12383.	13.7	19
286	Longâ€Lived Multifunctional Superhydrophobic Heterostructure Via Molecular Selfâ€Supply. Advanced Materials Interfaces, 2016, 3, 1500727.	3.7	19
287	Significant Enhancement of Single-Walled Carbon Nanotube Based Infrared Photodetector Using PbS Quantum Dots. IEEE Journal of Selected Topics in Quantum Electronics, 2018, 24, 1-8.	2.9	19
288	Investigation of black phosphorus as a nano-optical polarization element by polarized Raman spectroscopy. Nano Research, 2018, 11, 3154-3163.	10.4	19

#	ARTICLE	IF	CITATIONS
289	Anomalous Thermal Decomposition Behavior of Polycrystalline LiNi _{0.8} Mn _{0.1} Co _{0.1} O ₂ in PEOâ€Based Solid Polymer Electrolyte. Advanced Functional Materials, 2022, 32, .	14.9	19
290	A Common Tracking Software Project. Computing and Software for Big Science, 2022, 6, 1.	2.9	19
291	Magnetic Dirac fermions and Chern insulator supported on pristine silicon surface. Physical Review B, 2016, 94, .	3.2	18
292	A Mixedâ€Extractor Strategy for Efficient Sorting of Semiconducting Singleâ€Walled Carbon Nanotubes. Advanced Materials, 2017, 29, 1603565.	21.0	18
293	Boron oxides under pressure: Prediction of the hardest oxides. Physical Review B, 2018, 98, .	3.2	18
294	Measurement of complex optical susceptibility for individual carbon nanotubes by elliptically polarized light excitation. Nature Communications, 2018, 9, 3387.	12.8	18
295	Nucleation and dissociation of methane clathrate embryo at the gas–water interface. Proceedings of the United States of America, 2019, 116, 23410-23415.	7.1	18
296	<mml:math xmlns:mml="http://www.w3.org/1998/Math/MathML"><mml:msub><mml:mi mathvariant="normal">MgB<mml:mn>4</mml:mn></mml:mi </mml:msub></mml:math> trilayer film: A four-gap superconductor. Physical Review B, 2020, 101, .	3.2	18
297	Mixed-Dimensional Vertical Point p <i>–</i> n Junctions. ACS Nano, 2020, 14, 3181-3189.	14.6	18
298	Firstâ€principles dynamics of photoexcited molecules and materials towards a quantum description. Wiley Interdisciplinary Reviews: Computational Molecular Science, 2021, 11, e1492.	14.6	18
299	Aptamer-Functionalized Microdevices for Bioanalysis. ACS Applied Materials & Interfaces, 2021, 13, 9402-9411.	8.0	18
300	Complete structural characterization of single carbon nanotubes by Rayleigh scattering circular dichroism. Nature Nanotechnology, 2021, 16, 1073-1078.	31.5	18
301	Tunable electron-phonon coupling superconductivity in platinum diselenide. Physical Review Materials, 2017, 1, .	2.4	18
302	Orbital Dependence in Single-Atom Electrocatalytic Reactions. Journal of Physical Chemistry Letters, 2022, 13, 5969-5976.	4.6	18
303	Lattice-directed growth of single-walled carbon nanotubes with controlled geometries on surface. Carbon, 2012, 50, 3295-3297.	10.3	17
304	Silicene: from monolayer to multilayer — A concise review. Chinese Physics B, 2015, 24, 086102.	1.4	17
305	Strong-coupled hybrid structure of carbon nanotube and MoS ₂ monolayer with ultrafast interfacial charge transfer. Nanoscale, 2019, 11, 17195-17200.	5.6	17
306	Chloroformâ€Assisted Rapid Growth of Vertical Graphene Array and Its Application in Thermal Interface Materials. Advanced Science, 2022, 9, e2200737.	11.2	17

#	Article	IF	CITATIONS
307	Nanobarrier-terminated growth of single-walled carbon nanotubes on quartz surfaces. Nano Research, 2009, 2, 768.	10.4	16
308	Synthesis and Assembly of a Difunctional Core POM Cluster with Two Appended POM Cluster Caps. Chemistry - A European Journal, 2012, 18, 13596-13599.	3.3	16
309	Bis(pyrazol-1-yl)methane as Non-Chromophoric Ancillary Ligand for Charged Bis-Cyclometalated Iridium(III) Complexes. European Journal of Inorganic Chemistry, 2012, 2012, 3209-3215.	2.0	16
310	Extreme nonlinear strong-field photoemission from carbon nanotubes. Nature Communications, 2019, 10, 4891.	12.8	16
311	Water nanostructure formation on oxide probed in situ by optical resonances. Science Advances, 2019, 5, eaax6973.	10.3	16
312	Improving Photovoltaic Stability and Performance of Perovskite Solar Cells by Molecular Interface Engineering. Journal of Physical Chemistry C, 2019, 123, 1219-1225.	3.1	16
313	Carbon nanotube: Controlled synthesis determines its future. Science China Materials, 2020, 63, 16-34.	6.3	16
314	Helicityâ€resolved resonant Raman spectroscopy of layered WS ₂ . Journal of Raman Spectroscopy, 2021, 52, 525-531.	2.5	16
315	Atomically Precise Engineering of Singleâ€Molecule Stereoelectronic Effect. Angewandte Chemie - International Edition, 2021, 60, 12274-12278.	13.8	16
316	Low lattice thermal conductivity and good thermoelectric performance of cinnabar. Physical Review Materials, 2017, 1, .	2.4	16
317	Ultrafast Internal Exciton Dissociation through Edge States in MoS ₂ Nanosheets with Diffusion Blocking. Nano Letters, 2022, 22, 5651-5658.	9.1	16
318	Optical properties of clusters and molecules from real-time time-dependent density functional theory using a self-consistent field. Molecular Physics, 2010, 108, 1829-1844.	1.7	15
319	Observation of Low-Frequency Combination and Overtone Raman Modes in Misoriented Graphene. Journal of Physical Chemistry C, 2014, 118, 3636-3643.	3.1	15
320	Metal-film-assisted ultra-clean transfer of single-walled carbon nanotubes. Nano Research, 2014, 7, 981-989.	10.4	15
321	Global Photocurrent Generation in Phototransistors Based on Singleâ€Walled Carbon Nanotubes toward Highly Sensitive Infrared Detection. Advanced Optical Materials, 2019, 7, 1900597.	7.3	15
322	Doping modulated in-plane anisotropic Raman enhancement on layered ReS2. Nano Research, 2019, 12, 563-568.	10.4	15
323	Electric Field Tunable Ultrafast Interlayer Charge Transfer in Graphene/WS ₂ Heterostructure. Nano Letters, 2021, 21, 4403-4409.	9.1	15
324	Vertical Graphene Arrays as Electrodes for Ultraâ€High Energy Density AC Lineâ€Filtering Capacitors. Angewandte Chemie - International Edition, 2021, 60, 24505-24509.	13.8	15

#	Article	IF	CITATIONS
325	Modulusâ€Tailorable, Stretchable, and Biocompatible Carbonene Fiber for Adaptive Neural Electrode. Advanced Functional Materials, 2022, 32, 2107360.	14.9	15
326	High-Efficiency Selective Electron Tunnelling in a Heterostructure Photovoltaic Diode. Nano Letters, 2016, 16, 3600-3606.	9.1	14
327	Vibrational relaxation dynamics of the nitrogen-vacancy center in diamond. Physical Review B, 2018, 97,	3.2	14
328	Hard BN Clathrate Superconductors. Journal of Physical Chemistry Letters, 2019, 10, 2554-2560.	4.6	14
329	Toward attosecond control of electron dynamics in two-dimensional materials. Applied Physics Letters, 2020, 116, .	3.3	14
330	Holey Reduced Graphene Oxide Scaffolded Heterocyclic Aramid Fibers with Enhanced Mechanical Performance. Advanced Functional Materials, 2022, 32, .	14.9	14
331	Single-Walled Carbon Nanotubes Probing the Denaturation of Lysozyme. Journal of Physical Chemistry C, 2010, 114, 7717-7720.	3.1	13
332	Two-dimensional silicon-carbon hybrids with a honeycomb lattice: New family for two-dimensional photovoltaic materials. Science China: Physics, Mechanics and Astronomy, 2015, 58, 1.	5.1	13
333	CVD Growth of Carbon Nanotube Forest with Selective Wall-Number from Fe–Cu Catalyst. Journal of Physical Chemistry C, 2016, 120, 11163-11169.	3.1	13
334	Realâ€Time Observation of Carbon Nanotube Etching Process Using Polarized Optical Microscope. Advanced Materials, 2017, 29, 1701959.	21.0	13
335	Effect of Cation–π Interaction on Macroionic Selfâ€Assembly. Angewandte Chemie, 2018, 130, 4131-4136.	2.0	13
336	Phonon thermal transport in monolayer FeB2 from first principles. Computational Materials Science, 2018, 147, 132-136.	3.0	13
337	Carburization of Fe/Ni Catalyst for Efficient Growth of Singleâ€Walled Carbon Nanotubes. Small, 2019, 15, e1902240.	10.0	13
338	Growth of Singleâ€Walled Carbon Nanotubes with Different Chirality on Same Solid Cobalt Catalysts at Low Temperature. Small, 2019, 15, e1903896.	10.0	13
339	Reducing Anomalous Hysteresis in Perovskite Solar Cells by Suppressing the Interfacial Ferroelectric Order. ACS Applied Materials & Interfaces, 2020, 12, 12275-12284.	8.0	13
340	Growth of Homogeneous Highâ€Density Horizontal SWNT Arrays on Sapphire through a Magnesiumâ€Assisted Catalyst Anchoring Strategy. Angewandte Chemie - International Edition, 2021, 60, 9330-9333.	13.8	13
341	Inducing Transient Charge State of a Single Water Cluster on Cu(111) Surface. ACS Nano, 2016, 10, 4489-4495.	14.6	12
342	Scanning electron microscopy imaging of single-walled carbon nanotubes on substrates. Nano Research, 2017, 10, 1804-1818.	10.4	12

#	Article	IF	CITATIONS
343	A modified Wenzel model for water wetting on van der Waals layered materials with topographic surfaces. Nanoscale, 2017, 9, 3843-3849.	5.6	12
344	Engineering Dirac states in graphene: Coexisting type-I and type-II Floquet-Dirac fermions. Physical Review B, 2019, 99, .	3.2	12
345	Carbon fiber-promoted activation of catalyst for efficient growth of single-walled carbon nanotubes. Carbon, 2020, 156, 410-415.	10.3	12
346	Growth of high-density horizontal SWNT arrays using multi-cycle in-situ loading catalysts. Carbon, 2020, 157, 164-168.	10.3	12
347	Single-water-dipole-layer-driven Reversible Charge Order Transition in 1 <i>T</i> -TaS ₂ . Nano Letters, 2020, 20, 8854-8860.	9.1	12
348	Probing Laser-Induced Plasma Generation in Liquid Water. Journal of the American Chemical Society, 2021, 143, 10382-10388.	13.7	12
349	The helicity of Raman scattered light: principles and applications in two-dimensional materials. Science China Chemistry, 2022, 65, 269-283.	8.2	12
350	Observation of One-Dimensional Dirac Fermions in Silicon Nanoribbons. Nano Letters, 2022, 22, 695-701.	9.1	12
351	Quantum interference directed chiral raman scattering in two-dimensional enantiomers. Nature Communications, 2022, 13, 1254.	12.8	12
352	Highâ€Throughput Determination of Statistical Structure Information for Horizontal Carbon Nanotube Arrays by Optical Imaging. Advanced Materials, 2016, 28, 2018-2023.	21.0	11
353	Direct discrimination between semiconducting and metallic single-walled carbon nanotubes with high spatial resolution by SEM. Nano Research, 2017, 10, 1896-1902.	10.4	11
354	An Unprecedented Class of Benzoyldiazenidoâ€Functionalized Polyoxometalates with Enhanced Antitumour Activities. European Journal of Inorganic Chemistry, 2017, 2017, 5475-5484.	2.0	11
355	Investigation of Etching Behavior of Single-Walled Carbon Nanotubes Using Different Etchants. Journal of Physical Chemistry C, 2017, 121, 27655-27663.	3.1	11
356	Atomic-Scale Studies of Overlapping Grain Boundaries between Parallel and Quasi-Parallel Grains in Low-Symmetry Monolayer ReS2. Matter, 2020, 3, 2108-2123.	10.0	11
357	Visualizing molecular orientational ordering and electronic structure in CsnC60 fulleride films. Physical Review B, 2020, 101, .	3.2	11
358	Carbothermal shock enabled facile and fast growth of carbon nanotubes in a second. Nano Research, 2022, 15, 2576-2581.	10.4	11
359	Low lattice thermal conductivity and high figure of merit in nâ€ŧype doped <scp>fullâ€Heusler</scp> compounds X ₂ <scp>YAu</scp> (XÂ=ÂSr, Ba; YÂ=Âas, Sb). International Journal of Energy Research, 2021, 45, 20949-20958.	4.5	11
360	Automatic 3D image registration for nano-resolution chemical mapping using synchrotron spectro-tomography. Journal of Synchrotron Radiation, 2021, 28, 278-282.	2.4	11

#	Article	IF	CITATIONS
361	Spatially indirect intervalley excitons in bilayer <mml:math xmlns:mml="http://www.w3.org/1998/Math/MathML"> <mml:mrow> <mml:mi mathvariant="normal">W <mml:msub> <mml:mi>Se</mml:mi> <mml:mn>2</mml:mn> </mml:msub> Physical Review B, 2022, 105, .</mml:mi </mml:mrow></mml:math 	13.2 1ml:mrow:	> ¹ /mml:mat
362	Narrow-chirality distributed single-walled carbon nanotube synthesized from oxide promoted Fe–SiC catalyst. Carbon, 2022, 191, 146-152.	10.3	11
363	Quantum simulation of molecular interaction and dynamics at surfaces. Frontiers of Physics, 2011, 6, 294-308.	5.0	10
364	Free-Standing Single-Molecule Thick Crystals Consisting of Linear Long-Chain Polymers. Nano Letters, 2017, 17, 1655-1659.	9.1	10
365	Superconducting transition of FeSe / SrTiO3 induced by adsorption of semiconducting organic molecules. Physical Review B, 2017, 95, .	3.2	10
366	Optical Properties of Single- and Double-Functionalized Small Diamondoids. Journal of Physical Chemistry A, 2018, 122, 3583-3593.	2.5	10
367	Increasing the Density of Single-Walled Carbon Nanotube Arrays by Multiple Catalysts Reactivation. Journal of Physical Chemistry C, 2018, 122, 24823-24829.	3.1	10
368	Bifacial Raman Enhancement on Monolayer Two-Dimensional Materials. Nano Letters, 2019, 19, 1124-1130.	9.1	10
369	Phase Transition Photodetection in Charge Density Wave Tantalum Disulfide. Nano Letters, 2020, 20, 6725-6731.	9.1	10
370	Rapid synthesis of few-layer graphdiyne using radio frequency heating and its application for dendrite-free zinc anodes. 2D Materials, 2021, 8, 044003.	4.4	10
371	Engineering Three-Dimensional Moiré Flat Bands. Nano Letters, 2021, 21, 7519-7526.	9.1	10
372	Plasmon-Mediated CO ₂ Photoreduction via Indirect Charge Transfer on Small Silver Nanoclusters. Journal of Physical Chemistry C, 2021, 125, 26348-26353.	3.1	10
373	Ultra-low lattice thermal conductivity and anisotropic thermoelectric transport properties in Zintl compound β-K ₂ Te ₂ . Physical Chemistry Chemical Physics, 2022, 24, 4666-4673.	2.8	10
374	Tracking photocarrier-enhanced electron-phonon coupling in nonequilibrium. Npj Quantum Materials, 2022, 7, .	5.2	10
375	Calibrating Out-of-Equilibrium Electron–Phonon Couplings in Photoexcited MoS ₂ . Nano Letters, 2022, 22, 4800-4806.	9.1	10
376	Fe on Sb(111): Potential Two-Dimensional Ferromagnetic Superstructures. ACS Nano, 2017, 11, 2143-2149.	14.6	9
377	Investigation on the relationship between solubility of artemisinin and polyvinylpyrroli done addition by using DAOSD approach. Spectrochimica Acta - Part A: Molecular and Biomolecular Spectroscopy, 2017, 182, 136-142.	3.9	9
378	Band evolution of two-dimensional transition metal dichalcogenides under electric fields. Applied Physics Letters, 2019, 115, 083104.	3.3	9

#	Article	IF	CITATIONS
379	Giant photoinduced lattice distortion in oxygen vacancy ordered <mml:math xmlns:mml="http://www.w3.org/1998/Math/MathML"> <mml:msub> <mml:mi> SrCoO </mml:mi> <mml:mrow> < thin films. Physical Review B, 2019, 100, .</mml:mrow></mml:msub></mml:math 	ຠՠໄ ໝ າ>2.	5< />/ mml:mn>
380	Experimental observation of Dirac cones in artificial graphene lattices. Physical Review B, 2020, 102, .	3.2	9
381	The role of entrance functionalization in carbon nanotube-based nanofluidic systems: An intrinsic challenge. Physics of Fluids, 2021, 33, .	4.0	9
382	Deep-learning-based image registration for nano-resolution tomographic reconstruction. Journal of Synchrotron Radiation, 2021, 28, 1909-1915.	2.4	9
383	Controlling catalytic activity of gold cluster on MgO thin film for water splitting. Physical Review Materials, 2017, 1, .	2.4	9
384	Plasmon-mediated photodecomposition of NH3 via intramolecular charge transfer. Nano Research, 2022, 15, 3894-3900.	10.4	9
385	Unusual Deformation and Fracture in Gallium Telluride Multilayers. Journal of Physical Chemistry Letters, 2022, 13, 3831-3839.	4.6	9
386	Semiconductors: Growth of Large-Area 2D MoS2(1-x) Se2x Semiconductor Alloys (Adv. Mater. 17/2014). Advanced Materials, 2014, 26, 2763-2763.	21.0	8
387	The road to chirality-specific growth of single-walled carbon nanotubes. National Science Review, 2018, 5, 310-312.	9.5	8
388	Quartic anharmonicity and ultraâ€low lattice thermal conductivity of alkali antimonide compounds M 3 Sb (M = K, Rb and Cs). International Journal of Energy Research, 2021, 45, 6958-6965.	4.5	8
389	Growth of Semiconducting Singleâ€Walled Carbon Nanotubes Array by Precisely Inhibiting Metallic Tubes Using ZrO ₂ Nanoparticles. Small, 2021, 17, e2006605.	10.0	8
390	Comparison Study on Single Nucleotide Transport Phenomena in Carbon Nanotubes. Nano Letters, 2022, 22, 2147-2154.	9.1	8
391	Interaction of DNA with CNTs: Properties and Prospects for Electronic Sequencing. , 0, , 67-96.		7
392	<i>p</i> -Cu ₂ O/ <i>n</i> -ZnO Nanowires on ITO Glass for Solar Cells. Journal of Nanoscience and Nanotechnology, 2010, 10, 7473-7476.	0.9	7
393	A combined experimental and theoretical investigation of donor and acceptor interface in efficient aqueous-processed polymer/nanocrystal hybrid solar cells. Science China Chemistry, 2018, 61, 437-443.	8.2	7
394	Absorption, refraction and scattering retrieval in X-ray analyzer-based imaging. Journal of Synchrotron Radiation, 2018, 25, 1206-1213.	2.4	7
395	The excellent TE performance of photoelectric material CdSe along with a study of Zn(Cd)Se and Zn(Cd)Te based on first-principles. RSC Advances, 2019, 9, 25471-25479.	3.6	7
396	Quantum dynamics simulations: combining path integral nuclear dynamics and real-time TDDFT. Electronic Structure, 2019, 1, 044005.	2.8	7

#	Article	IF	CITATIONS
397	The structural, electronic and optic properties in a series of M2XY (M = Ga, In; X,Y = S, Se, Te) Janus monolayer materials based on GW and the Bethe-Salpeter equation. European Physical Journal B, 2020, 23, 1 Emergence of <mml:math< td=""><td>1.5</td><td>7</td></mml:math<>	1.5	7
398	xmlns:mml="http://www.w3.org/1998/Math/MathML"> <mml:mi>d</mml:mi> -orbital magnetic Dirac fermions in a <mml:math xmlns:mml="http://www.w3.org/1998/Math/MathML"><mml:mrow><mml:mi>Mo</mml:mi><mml:msub><mml:n mathvariant="normal">S<mml:mn>2</mml:mn></mml:n </mml:msub></mml:mrow></mml:math 	ni ^{3.2}	7
399	monolayer with squared pentagon structure. Physical Review B, 2020, 101, . Cellular processes involved in RAW 264.7 macrophages exposed to NPFF: A transcriptional study. Peptides, 2021, 136, 170469.	2.4	7
400	<i>In-Situ</i> Manipulation of the Magnetic Anisotropy of Single Mn Atom via Molecular Ligands. Nano Letters, 2021, 21, 3566-3572.	9.1	7
401	Strategies for Scalable Gas-Phase Preparation of Free-Standing Graphene. CCS Chemistry, 2021, 3, 1058-1077.	7.8	7
402	Vertical Graphene Arrays as Electrodes for Ultraâ€High Energy Density AC Lineâ€Filtering Capacitors. Angewandte Chemie, 2021, 133, 24710-24714.	2.0	7
403	Low lattice thermal conductivity and high figure of merit in p-type doped K ₃ IO*. Chinese Physics B, 2020, 29, 126501.	1.4	7
404	Probing Atomicâ€Scale Fracture of Grain Boundaries in Lowâ€symmetry 2D Materials. Small, 2021, 17, e2102739.	10.0	7
405	Creation of a novel inverted charge density wave state. Structural Dynamics, 2022, 9, 014501.	2.3	7
406	Solid supported ruthenium catalyst for growing single-walled carbon nanotubes with narrow chirality distribution. Carbon, 2022, 193, 35-41.	10.3	7
407	High-temperature fractional quantum Hall state in the Floquet kagome flat band. Physical Review B, 2022, 105, .	3.2	7
408	Subnanometer Single-Walled carbon nanotube growth from Fe-Containing Layered double hydroxides. Chemical Engineering Journal, 2022, 446, 137087.	12.7	7
409	A carbon nanotube-based sensing element. Optoelectronics Letters, 2007, 3, 81-84.	0.8	6
410	Sequential assembly of metal-free phthalocyanine on few-layer epitaxial graphene mediated by thickness-dependent surface potential. Nano Research, 2012, 5, 543-549.	10.4	6
411	trans-Dinitrosyl-Substituted Hexamolybdate and Study of Its Controllable NO Release. European Journal of Inorganic Chemistry, 2013, 2013, 1664-1671.	2.0	6
412	Enhancing the performance of poly(3-hexylthiophene)/ZnO nanorod arrays based hybrid solar cells through incorporation of a third component. Science China: Physics, Mechanics and Astronomy, 2014, 57, 1289-1298.	5.1	6
413	Prediction of silicon-based room temperature quantum spin Hall insulator via orbital mixing. Europhysics Letters, 2016, 113, 67003.	2.0	6
414	Reversible proton-switchable fluorescence controlled by conjugation effect in an organically-functionalized polyoxometalate. Scientific Reports, 2016, 6, 27861.	3.3	6

#	Article	IF	CITATIONS
415	Selective sorting of metallic/semiconducting single-walled carbon nanotube arrays by â€~igniter-assisted gas-phase etching'. Materials Chemistry Frontiers, 2018, 2, 157-162.	5.9	6
416	Low transverse momentum track reconstruction based on the Hough transform for the BESIII drift chamber. Radiation Detection Technology and Methods, 2018, 2, 1.	0.8	6
417	Direct imaging of surface states hidden in the third layer of Si (111)-7 × 7 surface by <i>pz</i> -wave tip Applied Physics Letters, 2018, 113, .	3.3	6
418	Carbon nanotubes assisting interchain charge transport in semiconducting polymer thin films towards much improved charge carrier mobility. Science China Materials, 2019, 62, 813-822.	6.3	6
419	A comprehensive study of phonon thermal transport in 2D IV-VI semiconductors MX (M = Ge, Sn; X = S,) Tj ETQq1	1.0.7843 2.1	14 rgBT /O
420	Plasmon-Induced Water Splitting on Ag-Alloyed Pt Single-Atom Catalysts. Frontiers in Chemistry, 2021, 9, 742794.	3.6	6
421	Either of Left–Right Hands Fits into an Identical Glove: A New Crystal of Polyoxometalate-Amino Acid Salt. Journal of Cluster Science, 2010, 21, 173-179.	3.3	5
422	Heterogeneous solvothermal synthesis of oneâ€dimensional titania nanostructures on transparent conductive glasses. Physica Status Solidi (A) Applications and Materials Science, 2011, 208, 2313-2316.	1.8	5
423	Preparation of Horizontal Single-Walled Carbon Nanotubes Arrays. Topics in Current Chemistry, 2016, 374, 85.	5.8	5
424	Atomic Layers: Tellurium-Assisted Epitaxial Growth of Large-Area, Highly Crystalline ReS2 Atomic Layers on Mica Substrate (Adv. Mater. 25/2016). Advanced Materials, 2016, 28, 5018-5018.	21.0	5
425	New sensitizers containing amide moieties as electron-accepting and anchoring groups for dye-sensitized solar cells. RSC Advances, 2016, 6, 74039-74045.	3.6	5
426	Highâ€Efficiency Photovoltaic Conversion at Selective Electron Tunneling Heterointerfaces. Advanced Electronic Materials, 2017, 3, 1700211.	5.1	5
427	Real-Space Imaging of Orbital Selectivity on SrTiO ₃ (001) Surface. ACS Applied Materials & Interfaces, 2019, 11, 37279-37284.	8.0	5
428	Dynamic defect as nonradiative recombination center in semiconductors. Physical Review B, 2019, 100, .	3.2	5
429	Local modulation of excitons and trions in monolayer WS2 by carbon nanotubes. Nano Research, 2020, 13, 1982-1987.	10.4	5
430	Determining the Oblique Angle of Vertical Graphene Arrays Using Helicity-Resolved Raman Spectroscopy. Journal of Physical Chemistry C, 2021, 125, 8353-8359.	3.1	5
431	Spatially Confined CVD Growth of Highâ€Density Semiconducting Singleâ€Walled Carbon Nanotube Horizontal Arrays. Advanced Functional Materials, 2022, 32, 2106643.	14.9	5
432	Inspecting the nonbonding and antibonding orbitals in a surface-supported metal–organic framework. Chemical Communications, 2021, 57, 4580-4583.	4.1	5

#	Article	IF	CITATIONS
433	Intrinsic Wettability in Pristine Graphene (Adv. Mater. 6/2022). Advanced Materials, 2022, 34, .	21.0	5
434	Traversing Double-Well Potential Energy Surfaces: Photoinduced Concurrent Intralayer and Interlayer Structural Transitions in XTe ₂ (X = Mo, W). ACS Nano, 2022, 16, 11124-11135.	14.6	5
435	Fabrication of metal suspending nanostructures by nanoimprint lithography (NIL) and isotropic reactive ion etching (RIE). Science in China Series D: Earth Sciences, 2009, 52, 1181-1186.	0.9	4
436	Preparation of Al-doped ZnO nanocrystalline aggregates with enhanced performance for dye adsorption. Science China: Physics, Mechanics and Astronomy, 2012, 55, 1198-1202.	5.1	4
437	Nanotube Arrays: Sorting out Semiconducting Singleâ€Walled Carbon Nanotube Arrays by Washing off Metallic Tubes Using SDS Aqueous Solution (Small 8/2013). Small, 2013, 9, 1305-1305.	10.0	4
438	Dye-sensitized solar cells: Atomic scale investigation of interface structure and dynamics. Chinese Physics B, 2014, 23, 086801.	1.4	4
439	Mechanism and modulation of terahertz generation from a semimetal - graphite. Scientific Reports, 2016, 6, 22798.	3.3	4
440	Universal Scaling of Intrinsic Resistivity in Twoâ€Đimensional Metallic Borophene. Angewandte Chemie, 2018, 130, 4675-4679.	2.0	4
441	Substrate-anchored solid solution catalysts for high density SWNTs growth. Carbon, 2018, 126, 313-318.	10.3	4
442	Reply to "Comment on " <i>Ab initio</i> evidence for nonthermal characteristics in ultrafast laser meltingâ€â€‰â€• Physical Review B, 2019, 99, .	3.2	4
443	Role of Explicitly Included Solvents on Ultrafast Electron Injection and Recombination Dynamics at TiO ₂ /Dye Interfaces. ACS Applied Materials & Interfaces, 2020, 12, 49174-49181.	8.0	4
444	High-Throughput Screening of Element-Doped Carbon Nanotubes Toward an Optimal One-Dimensional Superconductor. Journal of Physical Chemistry Letters, 2021, 12, 6667-6675.	4.6	4
445	Confined Fe Catalysts for Highâ€Đensity SWNT Arrays Growth: a New Territory for Catalystâ€Substrate Interaction Engineering. Small, 2021, 17, e2103433.	10.0	4
446	Electronically induced defect creation at semiconductor/oxide interface revealed by time-dependent density functional theory. Physical Review B, 2021, 104, .	3.2	4
447	Bi/Ti-phenolic network induced biomimetic synthesis of mesoporous hierarchical bimetallic hybrid nanocatalysts with enhanced visible-light photocatalytic performance. Colloids and Surfaces A: Physicochemical and Engineering Aspects, 2021, 629, 127518.	4.7	4
448	Viable substrates for the honeycomb-borophene growth. Physical Review Materials, 2021, 5, .	2.4	4
449	Complex Raman Tensor in Helicity-Changing Raman Spectra of Black Phosphorus under Circularly Polarized Light. Journal of Physical Chemistry Letters, 2022, 13, 1241-1248.	4.6	4
450	Ultrafast Electrochemical Capacitors with Carbon Related Materials as Electrodes for AC Line Filtering. Chemistry - A European Journal, 2022, 28, .	3.3	4

#	Article	IF	CITATIONS
451	Atomistic insights into plasmon induced water splitting. Science China: Physics, Mechanics and Astronomy, 2017, 60, 1.	5.1	3
452	Self-assembly of glycine on Cu(001): the effect of temperature and polarity. RSC Advances, 2017, 7, 4116-4123.	3.6	3
453	Anisotropic Ramanâ€Enhancement Effect on Singleâ€Walled Carbon Nanotube Arrays. Advanced Materials Interfaces, 2018, 5, 1700941.	3.7	3
454	Mechanical deformations of carbon nanorings: a study by molecular dynamics and nonlocal continuum mechanics. Meccanica, 2019, 54, 2281-2293.	2.0	3
455	Preparation of Mo2C–carbon nanomaterials for hydrogen evolution reaction. Carbon Letters, 2019, 29, 225-232.	5.9	3
456	Rotational and Vibrational Excitations of a Single Water Molecule by Inelastic Electron Tunneling Spectroscopy. Journal of Physical Chemistry Letters, 2020, 11, 1650-1655.	4.6	3
457	Renaissance of Oneâ€Ðimensional Nanomaterials. Advanced Functional Materials, 2022, 32, .	14.9	3
458	Bulk growth and separation of single-walled carbon nanotubes from rhenium catalyst. Nano Research, 2022, 15, 5775-5780.	10.4	3
459	Twist-Induced New Phonon Scattering Pathways in Bilayer Graphene Probed by Helicity-Resolved Raman Spectroscopy. Journal of Physical Chemistry C, 2022, 126, 10487-10493.	3.1	3
460	Molecular level interface designs using self-assembling technique for stabilizing Langmuir-Blodgett films. Zeitschrift Fur Elektrotechnik Und Elektrochemie, 1997, 101, 1113-1120.	0.9	2
461	CO2 mitigation in coal gasification cogeneration systems with integration of the shift reaction, CO2 absorption and methanol production. Journal of Thermal Science, 2004, 13, 193-198.	1.9	2
462	Synthesis, Characterization and Structure of [Fe(2,2′-bipy)3]2[α-Mo8O26]: An α-Octamolybdate-Supported Compound Formed During the Diffuse Process. Journal of Cluster Science, 2010, 21, 181-186.	3.3	2
463	Combining superior surface enhanced Raman scattering and photothermal conversion on one platform: a strategy of ill-defined gold nanoparticles. RSC Advances, 2015, 5, 27120-27125.	3.6	2
464	Investigation on the trioctylphosphine oxide-based super-concentrated HCl system. Spectrochimica Acta - Part A: Molecular and Biomolecular Spectroscopy, 2015, 136, 288-294.	3.9	2
465	Nucleophilic substitution reaction for rational post-functionalization of polyoxometalates. New Journal of Chemistry, 2016, 40, 906-909.	2.8	2
466	First-principles study of phonon thermal transport in II–VI group graphenelike materials. Journal of Vacuum Science and Technology A: Vacuum, Surfaces and Films, 2020, 38, 062202.	2.1	2
467	Unravelling a Zigzag Pathway for Hot Carrier Collection with Graphene Electrode. Journal of Physical Chemistry Letters, 2021, 12, 2886-2891.	4.6	2
468	Ultra-low lattice thermal conductivity and high thermoelectric efficiency of K3AuO. Journal of Applied Physics, 2021, 130, 045101.	2.5	2

#	Article	IF	CITATIONS
469	Epitaxial growth and band structure of antiferromagnetic Mott insulator CeOI. Physical Review Materials, 2020, 4, .	2.4	2
470	Passivation of Transition Metal Dichalcogenides Monolayers with a Surface onfined Atomically Thick Sulfur Layer. Small Structures, 2022, 3, .	12.0	2
471	Durably Self-Sustained Droplet on a Fully Miscible Liquid Film. Langmuir, 2022, 38, 3993-4000.	3.5	2
472	Simultaneous switching of supramolecular chirality and organizational chirality driven by Coulomb expansion. Nano Research, 0, , 1.	10.4	2
473	Brillouin Light Scattering of Halide Double Perovskite. Advanced Photonics Research, 2022, 3, .	3.6	2
474	Abnormal intensity and polarization of Raman scattered light at edges of layered MoS2. Nano Research, 2022, 15, 6416-6421.	10.4	2
475	An Incremental Approach to Efficiently Retrieving Representative Information for Mobile Search on Web. , 2010, , .		1
476	Rücktitelbild: Separation of Metallic and Semiconducting Single-Walled Carbon Nanotube Arrays by "Scotch Tape―(Angew. Chem. 30/2011). Angewandte Chemie, 2011, 123, 6804-6804.	2.0	1
477	Allâ€Silicon Switchable Magnetoelectric Effect through Interlayer Exchange Coupling. ChemPhysChem, 2017, 18, 1916-1920.	2.1	1
478	Highâ€Throughput Optical Imaging and Spectroscopy of Oneâ€Dimensional Materials. Chemistry - A European Journal, 2017, 23, 9703-9710.	3.3	1
479	Macroscopic superhydrophobicity achieved by atomic decoration with silicones. Journal of Chemical Physics, 2018, 149, 014706.	3.0	1
480	2D MoTe ₂ : Linear Dichroism and Nondestructive Crystalline Identification of Anisotropic Semimetal Few‣ayer MoTe ₂ (Small 44/2019). Small, 2019, 15, 1970239.	10.0	1
481	Superhydrophilic Graphdiyne: Superhydrophilic Graphdiyne Accelerates Interfacial Mass/Electron Transportation to Boost Electrocatalytic and Photoelectrocatalytic Water Oxidation Activity (Adv.) Tj ETQq1 1 0.	78146914 r	gB 1 /Overloc
482	Growth of Homogeneous Highâ€Density Horizontal SWNT Arrays on Sapphire through a Magnesiumâ€Assisted Catalyst Anchoring Strategy. Angewandte Chemie, 2021, 133, 9416-9419.	2.0	1
483	Accurate reconstruction algorithm for bilateral differential phase signals. Radiation Detection Technology and Methods, 2021, 5, 474-479.	0.8	1
484	Adaptive weighted total variation regularized phase retrieval in differential phase-contrast imaging. Optical Engineering, 2018, 57, 1.	1.0	1
485	Monitoring Strain-Controlled Exciton–Phonon Coupling in Layered MoS ₂ by Circularly Polarized Light. Journal of Physical Chemistry Letters, 2021, 12, 11555-11562.	4.6	1
486	Nonadiabatic electron-phonon coupling and its effects on superconductivity. Physical Review B, 2022, 105, .	3.2	1

#	Article	IF	CITATIONS
487	Fabrication and Structural Characterization of Azobenzene Monolayer on Silver Island Films By LB and SA Techniques. Molecular Crystals and Liquid Crystals, 1998, 314, 297-302.	0.3	0
488	Growth of Single-Walled Carbon Nanotubes on Surface with Controlled Structures. Materials Research Society Symposia Proceedings, 2009, 1204, 1.	0.1	0
489	Controlled synthesis of one-dimensional titania nanostructure films on transparent conductive glasses from a heterogeneous solvothermal method. , 2010, , .		0
490	Organic Fieldâ€Effect Transistors: Solutionâ€Processable, Lowâ€Voltage, and Highâ€Performance Monolayer Fieldâ€Effect Transistors with Aqueous Stability and High Sensitivity (Adv. Mater. 12/2015). Advanced Materials, 2015, 27, 2124-2124.	21.0	0
491	Frontispiece: Highâ€Throughput Optical Imaging and Spectroscopy of Oneâ€Dimensional Materials. Chemistry - A European Journal, 2017, 23, .	3.3	0
492	High throughput methods for evaluating the homogeneity of nanomaterials for nanoelectronics. , 2017, , .		0
493	Preliminary Study on High-sensitive Diffraction Enhanced Imaging at BSRF. Microscopy and Microanalysis, 2018, 24, 102-103.	0.4	0
494	Growth of Singleâ€Walled Carbon Nanotubes with Controlled Structure: Floating Carbide Solid Catalysts. Angewandte Chemie, 2020, 132, 10976-10979.	2.0	0
495	Local Kondo scattering in 4d-electron RuO _{<i>x</i>} nanoclusters on atomically-resolved ultrathin SrRuO ₃ films. Physical Chemistry Chemical Physics, 2021, 23, 22526-22531.	2.8	0
496	A gift to the Queen of Carbon: A special collection in honor and memory of Mildred Dresselhaus. Science Advances, 2021, 7, .	10.3	0
497	Calibrating the unphysical divergence in TDDFTÂ+ÂU simulations of a correlated oxide. Computational Materials Science, 2022, 203, 111167.	3.0	0
498	Spinâ€Glass State above Room Temperature in a Layered Nickelate La <i>_n</i> ₊₁ Ni <i>_n</i> O ₃ <i>_n</i> Advanced Electronic Materials, 2022, 8, .	u ba.1	0
499	Frontispiece: Ultrafast Electrochemical Capacitors with Carbon Related Materials as Electrodes for AC Line Filtering. Chemistry - A European Journal, 2022, 28, .	3.3	0